

Microtexturing of TiZrN-Coated Si₃N₄ cutting inserts for machining nickel alloy

Marina A. Volosova, Anna A. Okunkova*, Enver S. Mustafaev, Khasan I. Gkhashim, and Alexander P. Malakhinsky

Moscow State University of Technology “STANKIN”, Department of High-Efficiency Processing Technologies, Vadkovskiy per. 1, Moscow, 127994, Russia

Abstract. Insulating cutting ceramics exhibit outstanding mechanical and thermal properties but have electrical conductivity below the percolation threshold. It does not allow sophisticated shapes to be obtained by diamond grinding and polishing. The developed innovative technique is based on choosing the wear-resistant coating based on the chemical composition of the cutting ceramics and its behaviour at 1000–10 000°C, including changing the electrical conductivity from insulating to conducting level, dissociation/sublimation of its components and forming new conductive compounds during cooling that improves the conductive conditions in the interelectrode gap. Thus, the coating plays a wear-resistant role and serves as a technological asset in shaping methods based on the electrical destruction of the materials under discharges. TiZrN coating was deposited on a Si₃N₄ cutting insert using the vacuum-plasma method, with a thickness of 3.8–4.0 μm. The ceramics was microtextured by powder-mixed wire electrical discharge machining in TiO₂-suspension, $d_w = 0.25$ mm. The coated samples were subjected to adhesion and wear-resistance tests. Failure criterion in machining XH45MBTJuBP alloy was chosen a chamfer of 400 μm. The durability of the TiZrN-coated Si₃N₄ ceramic insert was improved by 1.33.

1 Introduction

The intensive wear of the tool edge during cutting heat-resistant alloys was under consideration by many scientific groups [1-3]. There are many ways to decrease the intensity of the mechanical and thermal stresses. However, one of the most effective ways to cut without reducing cutting speed and feed is microtexturing [4]. Mostly microtexturing the cutting edge has shown good results in enlarging the durability of the tool in turning mild steel [5], nickel superalloy [6], titanium alloy [7], and aluminum alloy [8] by a cutting tool made of hard alloy in the presence of a lubricant.

The microtexturing improves the tool's durability by decreasing forces and temperatures in the cutting area, residual stresses, and contact pad as a result of reducing friction forces. It also reduces the chemical interaction between the materials of the workpiece and tool and reduces the adhesion [9,10]. Si₃N₄ and other oxide and nitride ceramics meanwhile play a

* Corresponding author: a.okunkova@stankin.ru

more significant role in turning heat-resistant alloys due to their excellent ability to resist mechanical loads at high temperatures when the temperature on the contact pads can exceed 700°C [11,12].

The microtexture can be formed on a rake face by a convenient production method: laser processing [13], indentation [14], or electrical discharge technologies [15,16]. However, electrical discharge machining does not allow us removing material of the workpiece made of non-conductive ceramic such as oxides, some nitrides, and oxynitrides. The solution of the problem is in two main approaches – adding a conductive phase at the stage of sintering ceramics ($\text{Al}_2\text{O}_3+\text{TiC}$, $\text{Al}_2\text{O}_3+\text{SiC}$, $\text{Si}_3\text{N}_4+\text{TiN}$, $\text{SiAlON}+\text{TiN}$, etc.) that change as well the mechanical and physical properties of those ceramics [17-19] or using special assets to change the conductive properties of the ceramics surface and electrical conditions at the interelectrode gap by forming conducting debris during processing.

The last approach is based on thermochemistry theory and Gibb's law, taking into account the behaviour of materials heated above 1000°C. Introducing conductive coating and powder-mixed suspension allows the production of kerfs on the surface of the aluminum oxide of $54.16 \pm 0.05 \mu\text{m}$ in depth using Ni-Cr coating. The approach allowed the production of kerfs on the surface of Si_3N_4 ceramics using TiN coating [20]. The assisting electrode presents a conductive coating of the workpiece in the form of adhesive tape, PVD-coating, or their combination and is used for re-addressing the electrical impulses to the conductive components at the interelectrode gap, subjecting to thermal dissociation of the insulating workpiece material under layers [21]. Electrical discharge machining in powder-mixed suspension improves the discharge conditions between the tool and workpiece [22].

In the presented paper, the electrical discharge microtexturing was produced by a wire electrode made of annealed brass. Si_3N_4 cutting inserts were coated by the PVD method with the TiZrN coating, that were additionally coated by copper tape since TiZrN-coating exhibits threshold electrical conductivity despite its excellent wear-resistant properties. Microtextures were produced during immersion into the TiO_2 water-based suspension and that was proposed for the first time. The microtextures were controlled optically and using scanning electron microscopy. Adhesion and wear-resistance tests have completed the study.

2 Materials and methods

Si_3N_4 cutting inserts were taken as a research. The ANSI code is SNGN150716T02520 6190 (Sandvik Coromant, Sweden). The microtextures were produced on a 2-axis ARTA 123 Pro EDM machine (The Russian Federation). A $\varnothing 0.25\text{-mm}$ -wire tool was made of CuZn35 alloy. The current was $\sim 6\text{--}8$ A. The discharge frequency and pulse duration were varied during testing. A drawing of the cutting insert with microtextures and the cutting insert with an additional copper tape (HomaFix 404 with a width of 10 mm, Russia) mounted on the machine are shown in Figure 1.

The thickness of the copper tape was 0.035 ± 0.0002 mm. The machining was produced in the TiO_2 -suspension. Five microtextures were produced for each factors' set. The copper tape was used as an additional asset to improve the surface conductive properties and the electrical conditions in the gap. The textures were controlled optically on an Olympus BX51M instrument (Switzerland). The measurement error was calculated following [23]. Scanning electron microscopy (SEM) images in back-scattered (BSE) and secondary electron (SE) modes and chemical analysis of the microgrooves were provided on a TESCAN Mira 3 instrument (The Czech Republic).

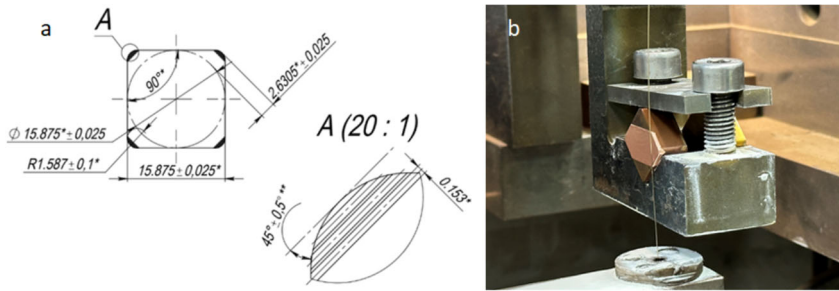


Fig. 1. Drawing of the square Si₃N₄-ceramic cutting insert with microtextures (a), the cutting insert mounted at the electrical discharge machine workspace (b).

TiO_x-271 powder (LLC "Titanium Investments", Russia), following GOST 9808-84, was added to the deionized water (Russia) with the concentration of 100 g/L. An average powder granule diameter was $d_{50} = 9.29\text{--}13.94\ \mu\text{m}$. The powder was pre-sifted on an AS200 machine (Germany) with an $\phi 10\text{-}\mu\text{m}$ -sieve. The suspension was prepared using the weight method on an EL104 balance (USA). The suspension was stirred on an IL100-6/1 ultrasonic machine (The Russian Federation) at 22 kHz (30 kHz – 1 MHz is destructive to biological organisms due to the formation of vapor-filled cavities in the liquid). The specimens were treated in a base dissolved in water following the experiments.

A wear-resistant TiZrN film of 3.8–4.0 μm were deposited on the cutting inserts using a unique unit developed in MSUT Stankin (The Russian Federation) providing purifying, coating deposition and chemical vapor deposition. The factors are provided in [24]. The inserts were pre-purified in an ultrasonic machine. The thickness was measured by a Calowear unit (USA). The adhesion strength was measured on a Nanovea M1 unit (USA) using ASTM C1624-05 standard.

A workpiece was a cylinder of XH45MBTJuBP nickel alloy (GOST 5632-2014) of $\phi 100\ \text{mm}$ turned on a ZMM CU500MRD machine (Bulgaria) with speed V of 300 m/min, feed s of 0.5 mm/rev, and depth t of 0.3 mm. Each specimen was tested 10 times. The flank wear pad was measured optically each 2 min on a Stereo Discovery V12 Zeiss optical instrument (Germany). The criterion of failure was taken at 400 μm .

3 Results and discussion

The coating was destructed under the load with the detected average value of L_{c1} of 2.46 N, L_{c2} of 10.87 N, and L_{c3} was not determined. The microtextures were $58\text{--}62 \pm 3\ \mu\text{m}$ in depth and $220\text{--}280 \pm 3\ \mu\text{m}$ and the coaxial distance of $280\text{--}320 \pm 3\ \mu\text{m}$ in width at $45 \pm 1^\circ$ to the symmetry axis on the rake face at $0.150\text{--}0.175 \pm 0.003\ \text{mm}$ of the edge.

The microphotograph of the obtained microgroove is shown in Figure 2, a. Microgrooves have no presence of drop-like oxide structures. There were no traces of tarnishing – effects of long-term thermal exposure along the edges of the formed microtexture – and as a result of thermochemical dissociation of the TiZrN-coating. It may mean that no thermochemical changes occurred in the structure of the surrounding coating during short-term thermal exposure of electric current pulses, and the wear-resistant properties of the coating are close to the initial ones – before microtexturing. SEM of the microtexture edge (Figure 2, b) shows the partial decomposition of the coating and under-layered ceramics and the presence of the secondary structure deposition. Chemical analyses of the secondary structures at the edge of the microgroove (Figure 2, c) demonstrated the elements corresponding to the chemical content of the ceramics, chosen coating, and powder suspension. It should be noted that the Zr element is not presented. It can be explained by the dissociation of Zr in the form of conductive particles at the discharge gap.

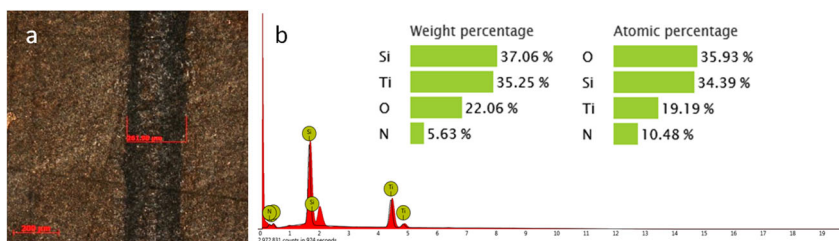


Fig. 2. Analyses of the produced microgrooves: microphotograph of the microgroove (a); the chemical analyses of the microtexture's edge (b).

Figure 3 presents the relations of flank chamfer of S_3N_4 -inserts with TiZrN coating in machining XH45MBTJuBP alloy for the inserts without microtextures and the inserts with microgrooves. The experimental results demonstrate that the durability of the S_3N_4 -insert with the coating was improved by 1.33. The average durability of the S_3N_4 -insert exceeded 8 min in machining the XH45MBTJuBP alloy.

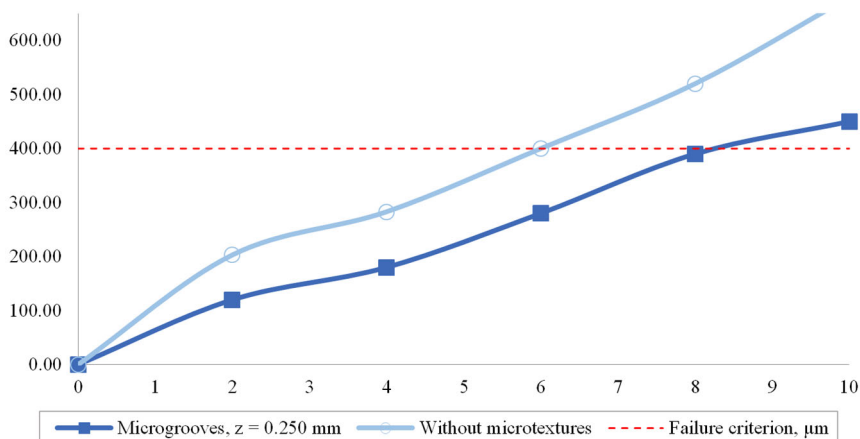


Fig. 3. Relation of the flank chamfer of S_3N_4 cutting inserts with TiZrN coating and the turning time in machining XH45MBTJuBP alloy.

4 Conclusion

The developed innovative assistance electrode technique during electrical discharge microtexturing included coating of the inserts with TiZrN wear-resistant coating and copper tape to improve the surficial electrical conductivity of the samples and machining in TiO_2 -mixed water-based suspension by brass wire tool electrode. The three microgrooves on each side of the cutting insert were on the rake faces of the inserts at 0.150–0.175 mm of the tool's edge. They were $\sim 250 \mu m$ wide and $\sim 60 \mu m$ depth, and the coaxial distance was $\sim 300 \mu m$. The microgrooves of the cutting tool made of S_3N_4 ceramics allows for increasing the durability of the tool in turning nickel-based alloy by a factor of 1.33. The durability of the insert without microtextures was 7.5 min.

This work was funded by the state assignment of the Ministry of Science and Higher Education of the Russian Federation, Project No. FSFS-2023-0003.

Data Availability Statement: The original contributions presented in the study are included in the article, further inquiries can be directed to the corresponding author.

References

1. P. Fernández-Lucio, G. Urbikain, S. Plaza, O. Pereira, *Eng. Sci. Technol. Int. J.* **54**, 101726 (2024).
2. A. Khramov, M. Gorchcov, N.K. Toan, E. Kiselev, *Mater. Res. Proc.* **21**, 122-126 (2022).
3. S.V. Fedorov, M.D. Pavlov, A.A. Okunkova, *J. Frict. Wear* **34**, 190-198 (2013).
4. X. Feng, X. Fan, J. Hu, J. Wei, *Lubricants* **11(6)**, 249 (2023).
5. J. Sun, Y. Zhou, J. Deng, J. Zhao, *Int. J. Adv. Manuf. Technol.* **86**, 3383-3394 (2016).
6. A. Rajurkar, S. Chinchankar, *Mater. Manuf. Processes* **39**, 529-545 (2023).
7. Z. Wu, J. Deng, C. Su, C. Luo, D. Xia, *Int. J. Refract. Met. Hard. Mater.* **45**, 238-248 (2014).
8. S. Musavi, M. Sepehriki, B. Davoodi, Se. Ali Niknam, *Int. J. Adv. Manuf. Technol.* **119**, 3343-3362 (2022).
9. D. Jianxin, W. Ze, L. Yunsong, Q. Ting, C. Jie, *Int. J. Refract. Met. Hard Mater.* **30**, 164-172 (2012).
10. S. Saketi, S. Odelros, J. Östby, M. Olsson, *Mater.* **12**, 2822 (2019).
11. V.V. Zakorzhevskii, V.E. Loryan, *Inorg. Mater.* **54**, 434-436 (2018).
12. K. Xue, P. Chen, W. Liu, B. Zou, L. Li, W. Chen, X. Wang, Z. Xu, *Coat* **13**, 1483 (2023).
13. S. Yang, D. Yu, D. Wang, *Coat* **14**, 1458 (2024).
14. M. Stebulyanin, E. Ostrikov, M. Migranov, S. Fedorov, *Coat* **12**, 1906 (2022).
15. B. Singh, R. Sasi, S. Kanmani Subbu, B. Muralidharan, *J Braz. Soc. Mech. Sci. Eng.* **41**, 152 (2019). <https://doi.org/10.1007/s40430-019-1654-6>
16. P. Koshy, J. Tovey, *CIRP Ann. Manuf. Technol.* **60**, 153-156 (2011).
17. S. Shi, *Mater. Sci. Eng., A* **893**, 146117 (2024).
18. E. Gevorkyan, M. Rucki, S. Panchenko, *Mater.* **13**, 5195 (2020).
19. L.A. Díaz, M.A. Montes-Morán, P.Y. Peretyagin, Y.G. Vladimirov, A. Okunkova, J.S. Moya, R. Torrecillas, *J. Nanopartic. Res.* **6**, 2257 (2014).
20. Y. Fukuzawa, T. Tani, N. Mohri, *J. Ceram. Soc. Jpn.* **108**, 184-190 (2000).
21. Y.H. Liu, X.P. Li, R.J. Ji, L.L. Yu, H.F. Zhang, Q.Y. Li, *J. Mater. Process. Technol.* **208**, 245-250 (2008).
22. P. R. Dewan, P. K. Kundu, R. Phipon, *AIP Conf. Proc.* **2273**, 050075 (2020).
23. O.V. Zakharov, B.M. Brzhozovskii, *Meas. Tech.* **49**, 1094-1097 (2006).
24. S. Grigoriev, Y. Melnik, *A. Metel, Surf. Coat. Technol.* **156**, 44-49 (2002).